A Multi-Design Point Sizing Methodology for Environmental Control Systems

Mingxuan Shi*, Yu Cai*, Jonathan Gladin†, and Dimitri N. Mavris‡
Aerospace Systems Design Laboratory, School of Aerospace Engineering,
Georgia Institute of Technology, Atlanta, Georgia, 30332

The environmental control system, which is to provide cabin air supply, conditioning, and pressurization, is the largest consumer of the secondary power in the aircraft. The impacts of the environmental control system designs have been studied for a long time. However, there is not a clear design guideline for it. Many studies have designed or optimized the environmental control system for a single point which was important in terms of vehicle or mission fuel economy. Some other researchers chose the most critical condition for sizing, such as the hot day and ground condition, or hot day with one engine failed. Some research also pointed out that the cooling efficiency can be greatly influenced when operation point is far from its design point. Therefore, a design guideline of the environmental control system is needed. To fill this gap, this paper proposes a multi-design point sizing methodology which sizes the environmental control system based on performance requirements of multiple points instead of those for a single point. This methodology will guarantee that all the requirements through the mission will be satisfied, and the efficiency will not be influenced much when the operation condition moves.

I. Introduction

The environmental control system (ECS) in an aircraft performs the functions of cabin air supply, conditioning, and pressurization. The ECS regulates the compressed air through pressure valves and cools it by ram air, then supplies it to the cabin. The compressed air is either from the compressor stage of the engine, which is called engine bleed, as applied in most commercial aircraft, or from electrically driven compressors, as used in the Boeing 787, a More Electric Aircraft (MEA) [1]. The first type of ECS is called the pneumatic ECS and the second one is called the electrical ECS. In either type of these two ECS, non-propulsive power is consumed either through the engine bleed extraction or electrical power consumption. As previous study stated, the ECS is the largest consumer of non-propulsive power [2]. The ram air to cool the compressed air also contributes to the aircraft ram drag. In this way, the cooling efficiency of the ECS can greatly influence the engine and the aircraft performance. Therefore, A properly design of ECS is desired to improve the aircraft fuel economy.

The analysis, optimization, and architecture of the ECS have been studied by many research. Exergy-based method is a popular way for analysis and optimization of the ECS, which is to calculate the entropy generated by each system or subsystem, and then find the optimal design variables by minimizing the entropy generation through the system. Pellegrini [3] illustrated the potential of the exergy-based method by analyzing the ECS performance at the cruise point. Bender [4] integrated the exergy analysis into the evaluation of the ECS by analyzing the entropy generation through each component. Pérez-Grande [5] proposed an exergy-based optimization method for to determine the heat exchanger geometry characteristics and the ratio between the core ECS supply air and total supply air. Following this work, Leo [6] conducted an exergy-based thermoeconomic analysis through the constructed and optimized ECS model. Figliola [7] also applied an exergy-based approach to optimize the ECS at the cruise condition. All these mentioned studies were based on the performance at the cruise point, which did not consider the operation of the ECS at other mission points. However, it should be noted that the most critical operation condition of the ECS is the ground, hot-day condition, which requires the largest cooling capacity. Rancruel [8] conducted an optimization research on the aircraft thermal management system which took the ECS as the study example based on exergy approach. Instead of using objective at a single mission point, he optimized the ECS based on total weight and total fuel burn. However, many operation requirements and constraints in critical points were not taken into account, such as overheating, one engine

*Ph.D Student, ASDL, School of Aerospace Engineering, Georgia Tech, AIAA Student Member
†Research Engineer II, ASDL, School of Aerospace Engineering, Georgia Tech, AIAA Member
‡S.P. Langley Distinguished Regents Professor and Director of ASDL, Georgia Tech, AIAA Fellow

failure, water extraction, anti-freezing, and etc. Parrilla [9] and Chakraborty [10] also evaluated the ECS architectures in terms of mission block fuel through mission analysis. Different from other research mentioned before, they took the most critical point in terms of cabin heat load, the ground, hot day condition, as the sizing point their studies. No matter the design point selected is the cruise condition or the ground, hot day condition, the ECS is sized using only one operation point, which is called Single-Design point (SDP) sizing methodology. ECS sized at the cruise point may not be able to handle the cooling requirement for a ground, hot day condition, while the ECS sized on ground may also have sub-optimal performance through the mission which has been shown by Shi [11] that the efficiency of the turbomachinery in the air cycle machine (ACM) will be greatly degraded when the flight conditions are far off from its ground, hot day sizing point. Such pattern was also reflected in the mission analysis in Shi's another paper [12].

Therefore, there is a need for a sizing methodology to ensure the ECS to be able to operate efficiently through the whole mission as well as satisfying requirements for all mission points, such as the cooling capacity requirement for ground, hot day condition, the anti-freezing requirement of the supply air before the entry of the cabin, and etc. However, there is very few existing literature or guidelines that show how to realize the the performance requirements while satisfying the constraints. Zhang [13] discussed types of requirements the an ECS design should satisfy and also stated a shown ECS design process, however, no actual sizing approach or guidelines were presented. Two books by National Research Council [14, 15] provided specific standards that the ECS should obey, but they still did not provide any instructions on sizing of the ECS. Probably the manufacturers may have their own methods to size the ECS in terms of certain objectives as well as meeting multiple constraints, but such methods are held as secrets, which is like the design method held by engine manufacturers [16]. However, research for academic purposes on ECS still require a reasonable sizing method of the ECS.

To fill such a gap that a proper and publicly available ECS sizing approach is very hard to find , this paper proposes a multi-design point (MDP) sizing methodology for the ECS. This proposed method is inspired by the MDP sizing methodology for the gas turbine engine [16, 17], which was developed to overcome the deficiencies of SDP sizing method shown in other studies [18, 19]. The proposed MDP ECS sizing method is capable of obtaining an optimal ECS while satisfying all the performance and operation constraints. Such capability is achieved by allowing sizing different components at different operating conditions as well as adjusting the design space topography which is defined by requirements and constraints of multiple mission points. The adjustment of the design space is realized using Newton's Method [20] to convert the dependencies among design variables, performance requirements and constraints into a set of non-linear equations. The requirements and constraints are guaranteed to be satisfied by solving this set of non-linear equations.

In this paper, the MDP sizing process of the ECS is implemented in the Numerical Propulsion System Simulation (NPSS) environment [21], the current industry standard tool for propulsion system sizing and analysis, inside which there is already a library of component models that are suitable for the ECS modeling. NPSS is also capable to perform the Newton Method as stated before through its own solver setup. The design parameters of the ECS is obtained through optimization using Genetic Algorithm (GA). To reduce the computational cost in the optimization process, a surrogate model of the ECS is constructed using neural networks to predict the performance of the ECS.

This paper is organized as following: the ECS architecture of interest for this study is shown in Sec. II; the modeling methodology is presented in Sec. III; the SDP and MDP sizing method and the corresponding implementation are introduced and compared in Sec. IV; the approach to demonstrate the capability of the proposed MDP sizing method is introduced in Sec. VI; the optimization method as well as the determined the design variables for either SDP and MDP are discussed in Sec. V; the results and discussions are included in Sec. VII; and the conclusions and the future work are stated in Sec. VIII.

II. Environmental Control System Architecture for This Study

The overall ECS architecture used in this paper was developed in the authors' previous work [11], which is shown in Fig. 1. The overall ECS comprises four modules: the bleed port at the higher pressure compressor (HPC) stage of the gas turbine to supply air, an air management system (AMS) to pre-cool the bleed air, a air cycle machine (ACS) which is the core of the ECS to cool the supply air by ram air, and the cabin which requires cooling. The focus of this paper is on the sizing methodology of the ACS, therefore, sizing methods for the engine or the cabin will not be covered. The performance requirments and operation constraints considered in the proposed MDP methodology may include those on the engines, AMS, ACS, and the cabin, but only the design variables of the ACS are considered. Design variables from the other systems can be taken into account with further integration, but it is sufficient to demonstrate the capability of the proposed sizing method using the ACS since the performance of the ECS is mainly determined by the ACS design.

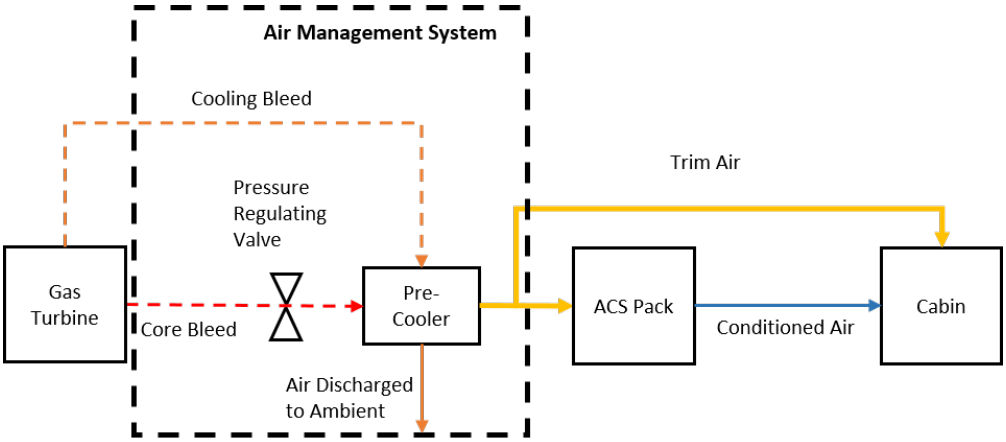

Fig. 1 Overall ECS architecture [11]

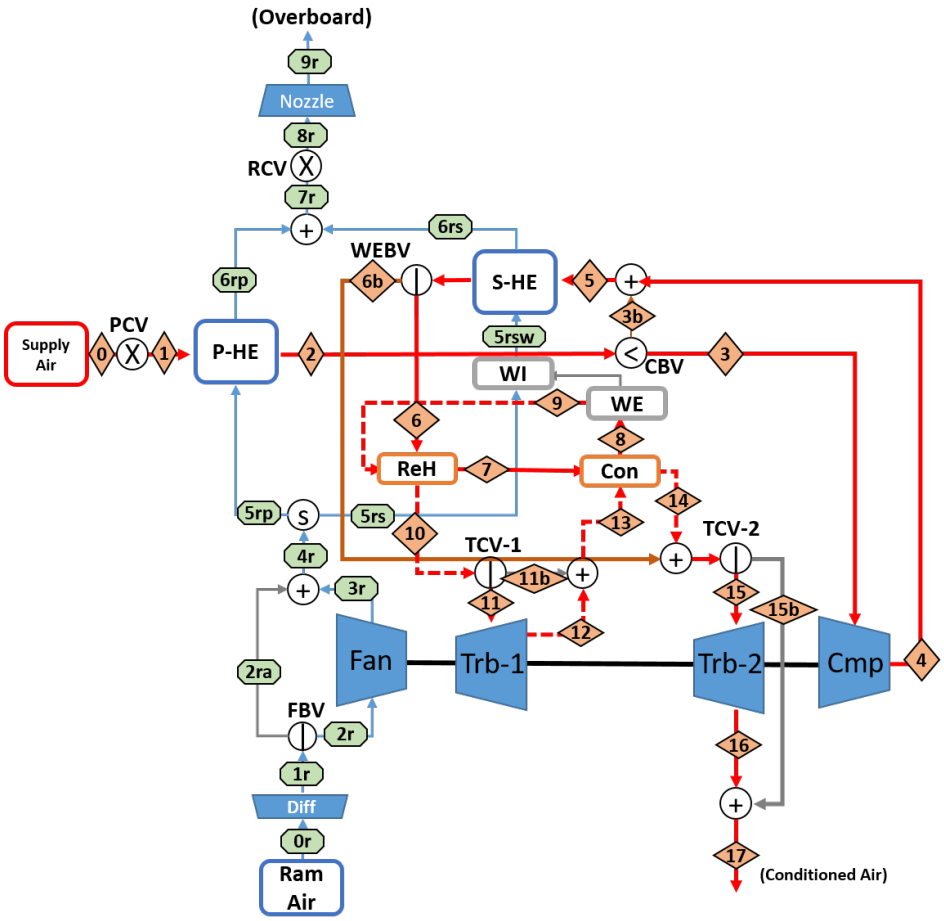

Fig. 2 Architecture of the ACS in the ECS [11]

The ACS in this paper is a four-wheel condensing ACS [22]. The architecture is illustrated in Fig. 2. In this ECS architecture, the supplied air from the pre-cooled engine bleed firstly is cooled by the ram air in the primary heat exchanger (P-HE), then is compressed by the compressor (Cmp), and then it passes the secondary heat exchanger (S-HE) for further cooling. After exiting the S-HE, the supply air passes through the water extraction loop to reduce its humidity. The water extraction loop comprises a reheater (ReH), a condenser (Con) and a water extractor (WE), and then it passes the turbine-1 (Trb-1) and turbine-2 (Trb-2) for expansion. After the expansion, the supply air finally is finally discharged from the ACS to perform cooling function. Two turbine control valves (TCV-1 and TCV-2) are used to control the work extraction from two turbines. It should be noted that before entering the cabin, the cooled supply air will be firstly mixed with recirculated air from the cabin in a mixing manifold. The mixing manifold is not shown here for simplicity, but it is modeled as part of the cabin.

III. Modeling Methodology

The model of each component in the ECS, the engine, and the cabin was constructed in the authors' previous work [11], where the details of the model can be found. This section will only briefly introduce component modeling that will influence the sizing of the ECS.

A. Standard NPSS Component Models

The standard component models are: duct, splitter, mixer, compressor, and the turbine. The duct is simply modeled by a fixed pressure drop. The splitter is modeled by a given bypass ratio at on-design mode, and mixer will thermodynamically mix two split flows. For off-design operation, the bypass ratio in the splitter will be changed to make the static pressure of the two streams in the mixer the same. The compressor and the turbine are modeled using the aerothermaldynamic model which is also called 0-D model, which can be found in many textbooks [23, 24]. They are modeled using a specified pressure ratio and efficiency for the on-design mode, which will be used to scale an existing off-design efficiency map to the sizing point. Then the operation point and the corresponding efficiency will be looked up during off-deisgn analysis. For all models above, the Mach number of entry and exit is given to size their corresponding areas. The weight of turbomachines is computed using power-to-weight ratio, and the weight of ducts are calculated by estimating the wall thickness, which was introduced by Shi [12].

B. Heat Exchanger Model

The heat exchanger model is constructed based on the number of transfer units (NTU) method based Kays and London's book [25]. At the on-design mode, the effectiveness and the pressure drops for both hot and cold streams are specified to size the geometric characteristics of the heat exchanger. At the off-design mode, the sized geometric characteristics are used to compute the effectiveness and the pressure drops. The volume of the heat exchanger (V_{hx}) and the volume of the flow (V_{flow}) are calculated by using the frontal area, flow area, and specified height, which are obtained also using the method in Kays and London's book [25]. The material volume can be estimated as $V_{\text{mat}} = V_{\text{hx}} - V_{\text{flow}}$. Then the mass is computed by $m_{\text{hx}} = \rho V_{\text{mat}}$ where ρ is the material density for the heat exchanger.

C. Cabin Heat Load

The cabin will not be sized through the implementation of the proposed MDP sizing methodology. However, the heat load requirement generated from the cabin will pose critical requirement of cooling capacity on the ECS. The cabin heat load requirement is modeled by assuming the cabin is is a steady state thermal equilibrium where all the generated heat equals the heat loss at all time so that the cabin temperature is maintained as specified. The heat loads modeled inside the cabin are metabolic heat from occupants and heat generated from electronic equipment. The convection, conduction, and radiation of the cabin with the environment is also modeled, as well as the solar radiation. The overall model can be represented in Fig. 3.

IV. Single-Design Point and Multi-Design Point Sizing Methodology for ECS

A. Single-Design Point Sizing Methodology for ECS

The SDP sizing methodology is to simply size ECS at a single operation condition such as the cruise condition, or the ground, hot day condition, or other user specified conditions. With a selected set of design variables, the components

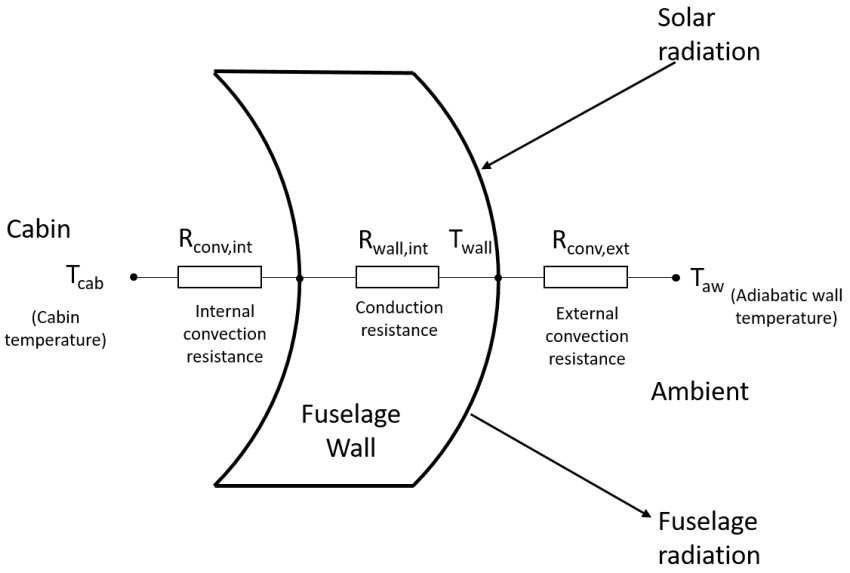

Fig. 3 Cabin heat transfer relation

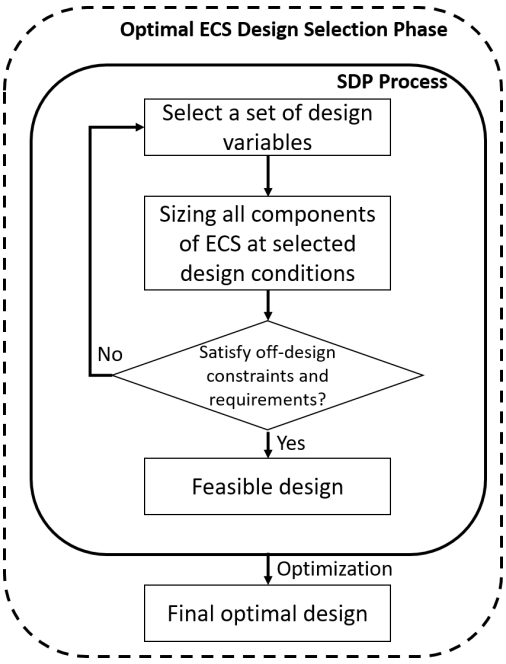

Fig. 4 Overview of the SDP sizing methodology for the ECS

of the ECS are sized at the design condition. The requirements and constraints will then be tested through off-design analysis using the sized ECS. If certain requirements and constraints are violated, then the design variables will be varied and the off-design analysis will be repeated to check if all requirements and constraints are satisfied. In this way a feasible design is produced. There are many techniques to select an optimal design of the ECS from the feasible candidate pool, and a general approach is mathematical optimization, which determines design variables by minimizing or maximizing the specified objectives. There are many mathematical optimization methods, and common ones are zero-order method, Newton's method, sequential quadratic programming, genetic algorithm, and etc. The designers may choose any of them based on the characteristics of the methodologies, the optimization problems, and their own experience conducting optimization. The optimization objectives can be chosen at multiple levels such as subsystem level, vehicle level, mission level, and etc. The subsystem-level metrics can be the ECS weight or required ram air at certain points. The vehicle-level metrics can be thrust specific fuel consumption (TSFC) at certain points. The mission-level metrics can be mission block fuel for designer-specified missions. This SDP sizing process can be summarized in Fig. 4.

B. Multi-Design Point Sizing Methodology for ECS

The fundamental idea of the Multi-Design Point Sizing Methodology for the ECS is to create a design space for ECS candidates where all the performance requirements and operation constraints are satisfied as well as allowing different components can be sized at different conditions. The optimal design of ECS is selected through optimization in the identified design space in terms of specified objectives. This fundamental idea is inspired by the MDP method for engine design [16, 17], but the actual methodology and implementation are different.

The MDP sizing process of the ECS is illustrated in Fig. 5. At the Requirements and Constraints Establish Phase, the requirements and constraints are identified in terms of the selected ECS architecture, standards, and the technology constraints. The design variables are also selected in this phase. At the Setup Phase, the established requirements and constraints are used to identify the sizing point for each component, and to formulate the non-linear equations which are used to enforce the satisfaction of the performance requirements and operation constraints. Such equations are also used to enforce the consistency among sizing parameters of components that are sized at different points. At the ECS Design Space Generation Phase, the formulated non-linear equations (NPSS solvers if using NPSS as the modeling environment), by solving which along the sizing process the design variables will be ensured to be in the feasible design range. A set of design of experiments of the design variables are selected to populate the design space through such a process. At the Optimal ECS Design Selection Phase, the optimal ECS designs are selected based on the designer-specified objectives from the design space which is populated by generated feasible designs.

1. Requirements and Constraints Establish Phase

At this phase, the design variables are firstly chosen based on the selected ECS architecture and modeling fidelity. For example, if the desired ECS architecture is a four-wheel condensing ECS as shown in this paper, the design variables may be chosen from design parameters of the compressor, two turbines, and the four heat exchangers. If modeling fidelity is low, the design variables may be selected to describe high-level performance such as pressure ratio of the compressor. If the desired modeling fidelity is high, the variables can be chosen to describe more detailed features such as the geometry parameters of the heat exchangers.

The performance requirements and operation constraints come from standards and technology limits. Standards may pose requirements that the ECS must obey to ensure safety in the ECS and comfort in the cabin, such as the temperature of the cold stream must be higher than 35 °F before entering the condenser [15], and the minimum amount of the fresh supply air is 0.55 lb/person/min as specified in Federal Aviation Administration (FAA) regulation [26]. The constraints posed by the technology may refer to the physical limitations of the components, such as the temperature of the ram air nozzle inlet and that of the compressor exit is limited by the material characteristics.

2. Setup Phase

At this phase, the detailed requirements and constraints are set up in terms of the model parameters. The corresponding design points along with the requirements and constraints are also identified. Then certain ECS parameters need to be varied to satisfy such requirements or constraints to form a feasible design space. Such properties derived from requirements and constraints that should be matched are called dependents in this context. The ECS parameters varied to match these dependents are call independents. Such relations can be formulated as a set of non-linear equations, where

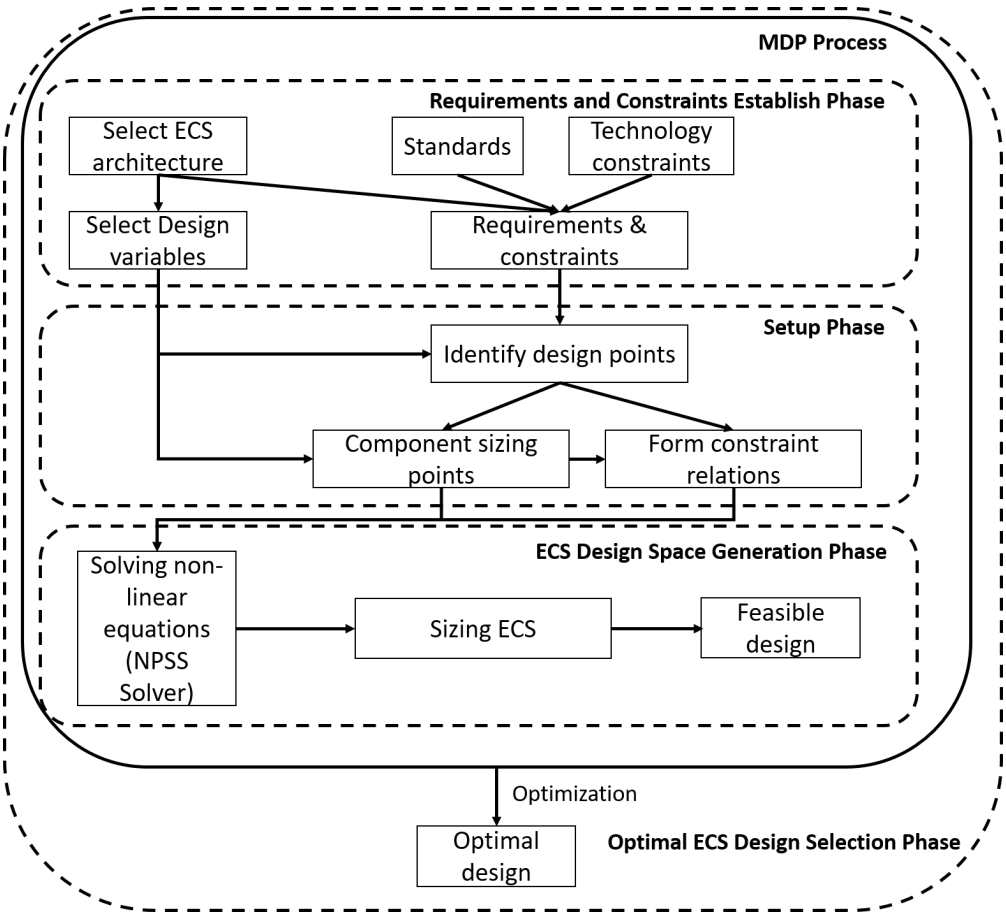

Fig. 5 Overview of the MDP sizing methodology for the ECS

the equations themselves are unknown. An example of the set of equations can be expressed in the following form:

$$\begin{aligned} F_1(\alpha_1, \alpha_2, \beta_1, \beta_2 \dots) &= 0 \\ F_2(\alpha_2, \beta_2, \beta_3 \dots) &= 0 \\ &\vdots \\ F_n(\dots \alpha_{n-1}, \alpha_n, \beta_{n-2} \dots) &= 0 \end{aligned}$$

where α's are the dependents and β's are the independents. One equation can have multiple dependents and independents, however, the total number of dependents n should be equal to the total number of independents. In this way, an $n \times n$ Jacobian matrix can be constructed to solve all the non-linear equations.

The requirements and the constraints can be either equality or inequality constraints. However, they are all expressed using the for of equality constraints. When the inequality constraints are not violated, the independents are set to the initial values. When the constraints are violated, the independents are varied to match limits set by the constraints. multiple constraints can be satisfied by varying the same number or fewer independents. The most stringent constraint is handled with highest priority, and in this way all the constraints are guaranteed satisfied through iteration of the solving process.

3. ECS Design Space Generation Phase

With the set independents and dependents at the previous phase, the non-linear equations are set and solved to find the feasible design at this phase. As executed in NPSS environment, the non-linear equations are set as NPSS solvers, which will be solved to find feasible independents for a given set of design variables during the sizing process.

Such independents will determine the sizing conditions for components, such as the mass flow, total pressure, total temperature, and etc.

4. Optimal ECS Design Selection Phase

Using the process stated before, a feasible design candidate can be discovered. With multiple sets of design variables, a pool of feasible designs can be identified. Then the same optimal design selection approach as in SDP sizing method such as mathematical optimization can be performed to select the optimal sets of design variables from the feasible design space. The optimization objectives can be also selected as the same as in SDP sizing method such as ECS weight, vehicle TSFC at certain operation conditions, or mission block fuel.

5. An Example of MDP Sizing Process

To understand the MDP process better, an simplified example is presented here to show how MDP works. Suppose that in the ECS of this example, the heat exchangers are sized at Point 1, all other components are sized at Point 2, and there is also a constraint that the ratio of corrected speed of compressor between point 2 and point 3 (which has the maximum compressor corrected speed) should should be smaller than the speed scalar in point 2 to avoid extrapolation when using off-design performance map. Meanwhile, the ECS pack discharge temperature should equal to the desired temperature which is calculated by the cabin model, which is controlled by adjusting the intake ram air. The simplified descriptions of formulated the equations can be presented as:

1) Varying amount of ram air $\dot{m}_{\text{ram}}$ at to meet the target discharge temperature T_{exit} for all points:

$$\begin{aligned} F_1(\dot{m}_{\text{ram,point1}}) - T_{\text{exit,point1}} &= 0 \\ F_2(\dot{m}_{\text{ram,point2}}) - T_{\text{exit,point2}} &= 0 \\ F_3(\dot{m}_{\text{ram,point3}}) - T_{\text{exit,point3}} &= 0 \end{aligned}$$

2) Enforcing sizing parameters of heat exchangers $Para_{\text{hx}}$ at point 2, and point 3 are consistent with the ones that are sized at point 1:

$$\begin{aligned} Para_{\text{hx,point2}} - Para_{\text{hx,point1}} &= 0 \\ Para_{\text{hx,point3}} - Para_{\text{hx,point1}} &= 0 \end{aligned}$$

3) Enforcing sizing parameters of components other than heat exchangers $Para_{\text{other}}$ at point 1, and point 3 are consistent with the ones that are sized at point 2:

$$\begin{aligned} Para_{\text{other,point1}} - Para_{\text{other,point2}} &= 0 \\ Para_{\text{other,point3}} - Para_{\text{other,point2}} &= 0 \end{aligned}$$

4) Ensuring the compressor corrected speed scalar des_{Nc}, which marks the position of the design scaling point on the map, at point 2 is smaller than the ratio of corrected speed of compressor between point 2 and point 3 $\frac{N_{\text{c,point2}}}{N_{\text{c,point3}}}$. It should be noted that this relation is still expressed as the equality form, but this equation is only active when this constraint is violated.

$$des_{Nc,point2} - \frac{N_{c,point2}}{N_{c,point3}} = 0$$

Then the model executes the ECS model at point 1, 2 and 3, in an iterative manner, until the equations are solved by varying the sizing parameters. The solving process can be understood as that the sizing parameters are varied to satisfy the the requirements and constraints, and the execution of the model at each certain point updates itself using the information from executions at other points until convergence.

C. Implementation

1. Design Variables

High-level parameters are chosen as the design variables since the desired modeling fidelity in this paper is low. The selected design variables are listed in Table 1:

Table 1 Selected Design Variables

Variable name	Explanation
Cmp.PR, π_{cmp}	Compressor pressure ratio
Trb1.PR, π_{trb1}	Turbine-1 pressure ratio
PrimHX.effect, η_{HX1}	Primary heat exchanger effectiveness
SecHX.effect, η_{HX2}	Secondary heat exchanger effectiveness
ReH.effect, η_{reh}	Reheater heat exchanger effectiveness
Con.effect, η_{con}	Condenser heat exchanger effectiveness

The design efficiency of the turbomachine can be expressed as a function of its sizing pressure ratio, and the design pressure drop of heat exchangers also depends on the sizing effectiveness, therefore, there is no need to include such parameters in the design variables. The pressure ratio of Trb-2 is determined by the turbomachine matching process which size the Trb-2 in terms of torque balance, as the pressure ratio of Trb-1 is specified as a design variable. Varying the pressure ratio of Trb-1 is the same as varying the work split ratio between Trb-1 and Trb-2 to design the two turbines. The sizing conditions for these components can be different, and the exact implementation in this study will be discussed later in Sec. IV.C.3. It should be noted that these design variables are not the exact variables that are used in the optimization.

2. Requirements, Constraints and Design Points

Typical performance requirements and operation constraints of the ECS along all mission points are selected here to demonstrate the capability of the MDP sizing method, of which the corresponding independents and dependents are listed and explained below:

Table 2 Performance Requirements and Operation Constraints

Independents	Dependents	Explanation
$\dot{W}_{\text{Supply\_Bleed}}$	$\dot{W}_{\text{Supply\_Cabin}}$	C1: Bleed extraction to ensure fresh cabin air $\geq 0.55\,\text{lb/person/min}$
$T_{\text{Discharge\_ECS}}$	$T_{\text{Supply\_Cabin}}$	C2: ECS pack discharge T to ensure Cabin supply T $\geq 40\,^{\circ}\text{F}$
BPR_{TCV-1}	$T_{\text{Conr\_Cold}}$	C3: TCV-1 bypass ratio to ensure condenser cold entry temperature $\geq 34\,^{\circ}\text{F}$
BPR_{TCV-2}	$T_{\text{Cmp\_Exit}}$	C4: TCV-2 bypass ratio to ensure Compressor exit temperature $\leq 260\,^{\circ}\text{F}$
BPR_{TCV-2}	$T_{\text{Ram\_Nozzle}}$	C5: TCV-2 bypass ratio to ensure ram air nozzle temperature $\leq 250\,^{\circ}\text{F}$

3. Design Points Selection

The components are sized at the points where they serve the most critical functions. Therefore, the heat exchangers should be sized at the ground, hot day condition with cabin fully occupied (Ground), since this condition poses the most critical cooling load to heat exchangers. The turbomachines should be sized at points with high corrected speed. To find out this point, an ECS using SDP sizing method on the ground, hot day condition is analyzed through selected mission points from takeoff to cruise. The corrected speed of compressor, Trb-1, and Trb-2 are plotted in Fig. 6(a) against altitude of the corresponding flight conditions. These corrected speeds are normalized by the corrected speed of the point at 31000 ft, which has the highest corrected speed in the cruise segment. It should be noted that the Mach number from takeoff to cruise is correlated with the flight altitude as illustrated in Fig. 6(b), therefore, a single altitude in Fig. 6(a) can uniquely identify a single mission point. From Fig. 6(a), it can be seen that the cruise condition has a higher corrected speed for all turbomachines compared to the ground condition. Considering this fact of high corrected speed as well as the cruise segment is the longest segment of the mission, the 31000-ft point of cruise segment (Cruise) is selected as the sizing point for turbomachines. It should be also noted that the maximum corrected speed is reached at the altitude around 10000 ft which is the middle of the climb (Mid-Climb), thus this point is selected to constrain the

position of the scaling normalized corrected speed at the cruise point to avoid extrapolation when using performance map during off-design analyses. This corrected speed constraint is denoted as C_{Nc} in this paper.

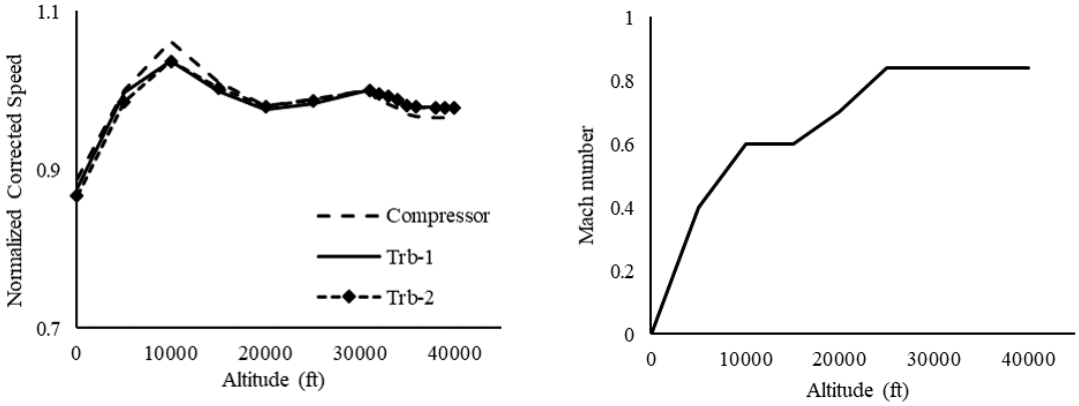

(a) Normalized corrected speeds of turbomachines (b) Selected mission points from takeoff to cruise

Fig. 6 Corrected speeds of turbomachines with corresponding flight conditions

Considering these three design points and all other requirements and constraints mentioned in Table 2, the sizing conditions can be summarized in Table 3, where the check mark after one point indicates a certain sizing requirements or constraints should be satisfied at this point. It should also be noted that the implementation discussed in this study is just to provide a typical example to demonstrate the MDP sizing methodology for the ECS. There could be many other options to select design points, design variables, requirements, constraints, and etc.

Table 3 Design Points Selection

Point	Cmp Sizing	Trb-1 Sizing	Trb-2 Sizing	HX Sizing	C_{Nc}	C1	C2	C3	C4	C5
Ground				✓		✓	✓	✓	✓	✓
Cruise	✓	✓	✓			✓	✓	✓	✓	✓
Mid-Climb					✓	✓	✓	✓	✓	✓

V. Optimization of Design Variables for SDP and MDP Sizing Methodology

A. Optimization Problem Setup

As a secondary power consuming subsystem, the ECS has an impact on vehicle-level performance through its mass contribution to vehicle empty weight, drag increment due to ram air intake, and fuel penalty due to secondary power extraction [10]. Therefore, it is natural to pose the ECS optimization problem as a multi-objective optimization problem. Since the number of occupants and dimensions of fuselage and cabin are held constant, the supply air requirement (i.e. pneumatic power extraction) at any given flight condition is invariant. Therefore, the objectives considered in this work are the mass of ECS pack (m_{pack}) and required ram air mass flow rate ($\dot{m}_{\text{ram}}$) at respective design condition, i.e. the ECS sized by SDP is optimized at the ground condition, while the ECS sized by MDP is optimized at the cruise condition even the heat exchangers are sized on ground. The ECS pack mass and the required ram air are considered conflicting objectives when being minimized simultaneously. This is because to reduce the required ram air, more heat has to be removed through the primary and secondary heat exchangers, which requires a high effectiveness of the heat exchangers as well as a high pressure ratio of the compressor. Higher effectiveness correlates with a higher pressure drop of the heat exchanger, indicating the heat transfer area is larger which leads to a larger volume and higher mass. As the pressure ratio of the compressor increases, the compressor loading increases which requires a larger and heavier compressor. At the same time, turbines also need to be larger to supply enough power to the compressor. Therefore, as the required ram air decreases, the minimum mass of the ECS pack is expected to increase. It should be noted that in

this study while the mass of ECS packs are being optimized, the mass of the ducts to supply cooling air to the cabin is assumed unchanged since the cabin cooling load is invariant.

The optimization problem is formally stated as follows, shared by both SDP and MDP methodologies. T^*_{exit} is the target discharge temperature of the ECS which is calculated by the cabin model based on the cabin cooling load which depends on the number of occupants and the operation conditions.

$$\begin{aligned} \underset{\mathbf{x}}{\text{minimize}} \quad & \begin{bmatrix} m_{\text{pack}}(\mathbf{x}) \\ \dot{m}_{\text{ram}} \end{bmatrix} \\ \text{subject to} \quad & T_{\text{exit}}(\mathbf{x}) - T^*_{\text{exit}} = 0, \\ & \mathbf{x} : [\eta_{\text{HX1}}, \eta_{\text{HX2}}, \eta_{\text{reh}}, \eta_{\text{con}}, \pi_{\text{cmp}}, \pi_{\text{trb1}}, \dot{m}_{\text{ram}}]^\intercal \in \text{[Table 4 intervals]} \end{aligned}$$

Table 4 Bounds of Design Variables

Design Variable	Lower Bound	Upper Bound
η_{HX1}	0.30	0.95
η_{HX2}	0.30	0.95
η_{reh}	0.30	0.59
η_{con}	0.30	0.80
π_{cmp}	1.05	2.00
π_{trb1}	1.05	3.00
$\dot{m}_{\text{ram}}$ (lbm/s)	1.00	8.00

B. Optimization Methodology

The Non-dominated Sorting Genetic Algorithm II (NSGA-II) [27, 28] is used to approach the Pareto frontier. Compared to other approaches which solve a multi-objective optimization problem by solving a set of single-objective problems using weighted aggregation function, the NSGA-II algorithm handles the original multi-objective optimization problem directly by operating on a population of design candidates and using genetic operators like cross-over, mutation, and selection to ensure that at each iteration a fraction of the population is non-dominated. When the algorithm converges, the remaining non-dominated members in the population are said to fall on the Pareto frontier.

Since the convergence of the analysis environment is sensitive to the initial values of the ECS model, efforts have to be made for finding proper initial guesses manually for certain design cases to converge. Therefore, it is impractical to evaluate the pack mass and discharge temperature directly using the analysis environment within the NSGA-II algorithm. Instead, surrogate models for pack mass and discharge temperature as functions of the design variables are created for both SDP and MDP methodologies. Table 5 presents the specification of Designs of Experiments used to sample the design space, from which single-layer neural network surrogate models are created, whose prediction errors are documented in Table 5 and Figs. 7-8. With root mean square errors less than 0.7%, the surrogate models are considered sufficiently good for the purpose of this optimization.

The NSGA-II algorithm is executed in MATLAB for both SDP and MDP methodologies with a population size of 500. At each generation, 20% of the population is selected from the non-dominated individuals, while the rest is selected from individuals with higher non-domination levels, i.e. the converged Pareto frontier contains 100 designs. The algorithm stops when the average change in the spread of Pareto front over the past 100 generations is less than 10^{-5} and the final spread is less than the mean spread over the past 100 generations.

C. Optimization Results

The optimization results for the ECS sized by SDP and MDP are shown in Figs. 9-10, respectively. The design decision is to pick the candidate that is closest to the ideal point which is defined as the virtual point at the minimum pack mass and minimum ram air flow determined from the Pareto frontier. In these two figures, the design decision point is the point with smallest normalized distance to ideal.

Table 5 Specifications of Designs of Experiments and Surrogate Models

	SDP	MDP
Training: Central composite design sampling	135	135
Training: Latin-hypercube design sampling	350	450
Validation: Random sampling	150	200
Neural network hidden layer structure	1 layer, 25x tanh	1 layer, 35x tanh
Residual distribution	See Fig. 7	See Fig. 8
RMSE of $\log m_{\text{pack}}$, training	2.505×10^{-3}	3.100×10^{-3}
RMSE of $\log m_{\text{pack}}$, validation	3.685×10^{-3}	4.063×10^{-3}
RMSE of $\log T_{\text{exit}}$, training	3.295×10^{-3}	4.531×10^{-3}
RMSE of $\log T_{\text{exit}}$, validation	5.894×10^{-3}	6.553×10^{-3}

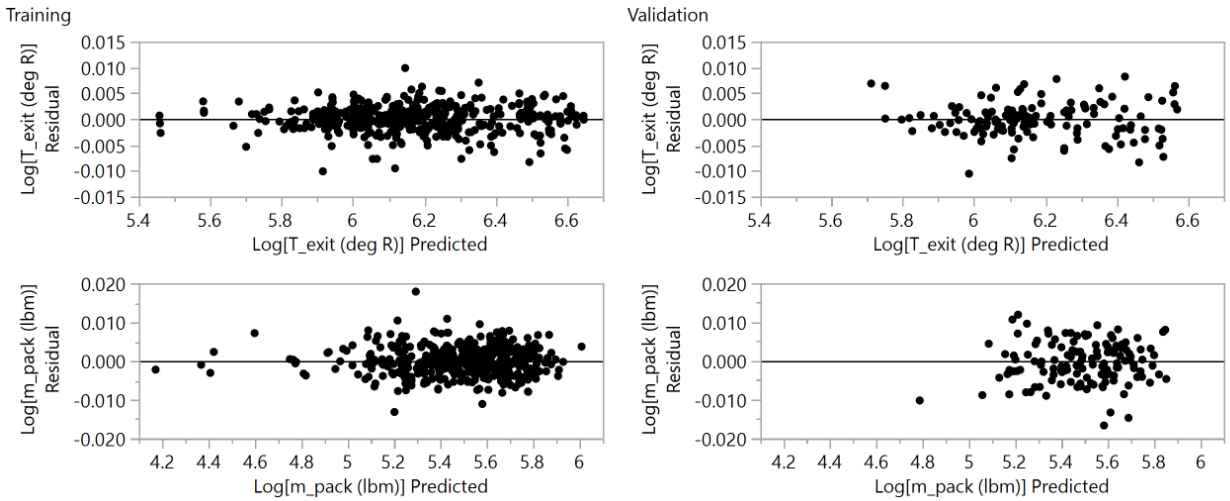

Fig. 7 Residual vs predicted plots for discharge temperature and pack mass from SDP surrogate model

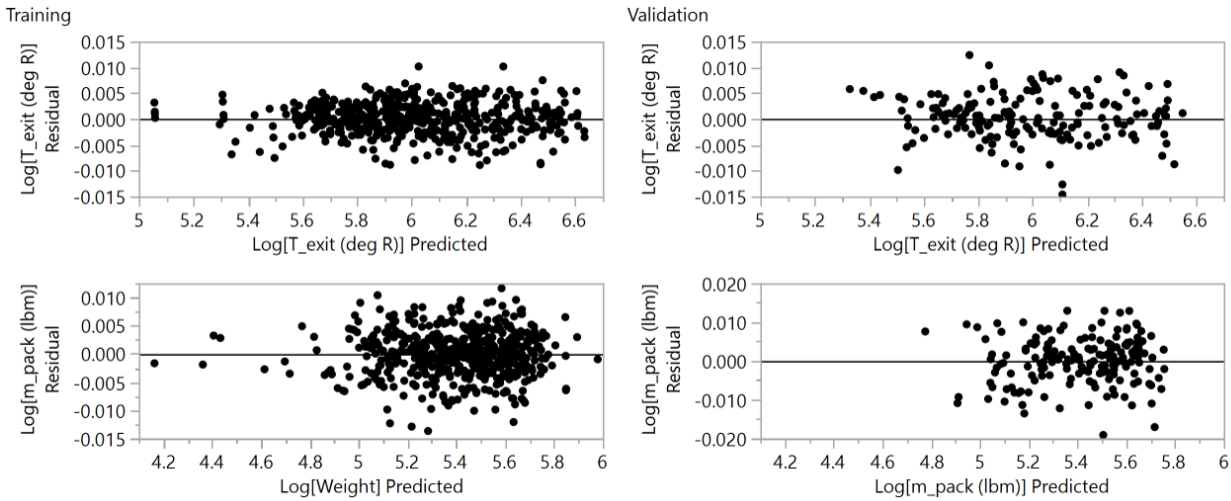

Fig. 8 Residual vs predicted plots for discharge temperature and pack mass from MDP surrogate model

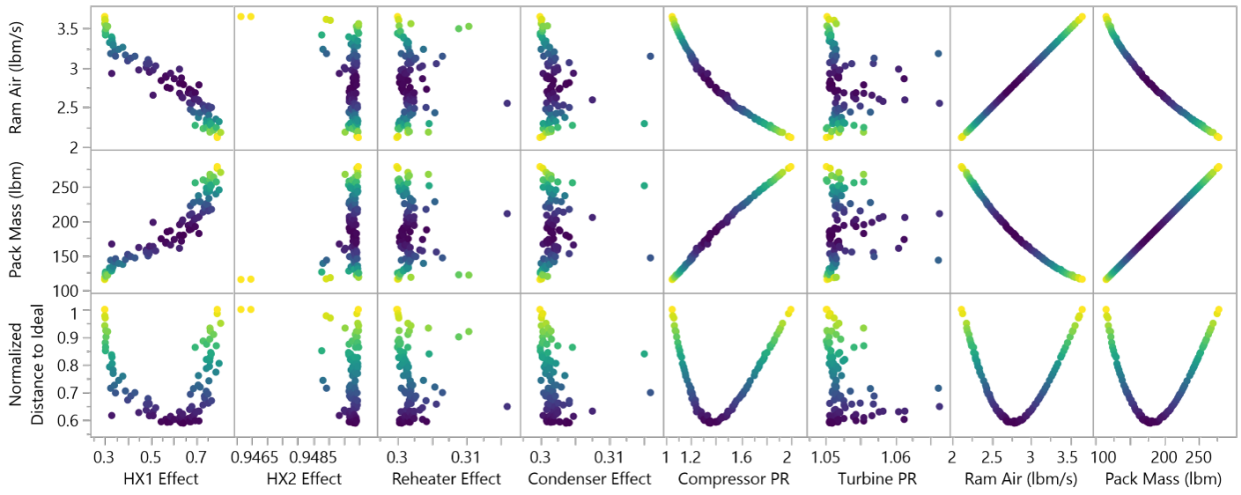

Fig. 9 Specifications of Pareto designs for SDP methodology

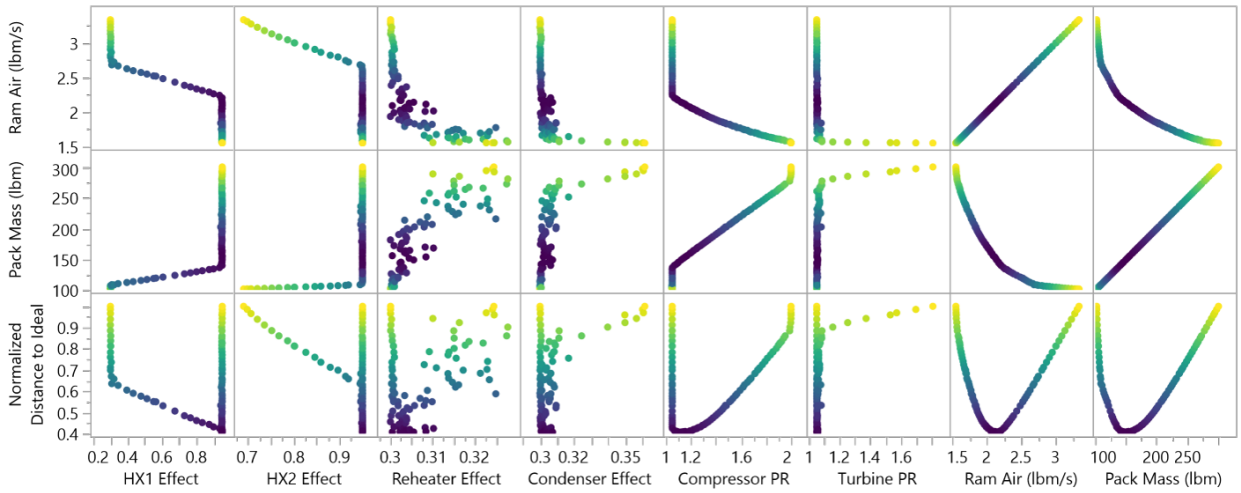

Fig. 10 Specifications of Pareto designs for MDP methodology

Comparing Figs. 9-10, the Pareto design space generated by the SDP sizing method is more scattered than that from MDP sizing method. This can be understood as that in MDP, some of the suboptimal points are already eliminated by sizing the components at different design points. This is also why MDP design variables have kinks at certain design values. It can be discovered that for both MDP and SDP design, the ram air decreases as the effectiveness of the primary heat exchanger increases, while the weight is increased as well. This is because as effectiveness increases less ram air is required to remove the same amount of heat, but the heat exchanger becomes bigger. One interesting finding here is that the effectiveness of the secondary heat exchanger tends to be clustered at the upper bound for SDP design. It should be noted here that all the points in the figures are of Pareto optimality. Therefore, such clustering feature means that only when the effectiveness of the secondary heat exchanger hits the upper limit, the Pareto optimality can be reached, indicating the this effectiveness is critical in SDP, which is optimized on ground where the cooling capacity of the ram air is lowest along the mission. Looking at the effectiveness of the secondary heat exchanger in MDP, points that are off the upper limit begin to appear. This is because the operation condition for the optimization is at high altitude where the ram air temperature is much lower than that on ground, making the heat transfer effectiveness less critical than using SDP. The reheater and condenser effectiveness for both SDP and MDP designs are clustered towards the lower limit, although some points in the MDP results are slightly off (still very close). This is because the effectiveness of reheater and condenser does not influence much on the required ram air; instead, it is to ensure that the temperature

inside the condenser is low enough to condense the water vapor, which is an internal constraint satisfied by the given lower effectiveness limits. Therefore, the Pareto optimality tends to reduce these two effectiveness to reduce the pack mass. Regarding the compressor pressure ratio, the trends for both SDP and MDP are the same: as the pressure ratio increases, the pack mass increases but the required ram air drops. The design pressure ratio with shortest normalized distance to the ideal point of MDP is smaller than that of SDP, because at high altitude it does not require as higher pressure ratio as on ground to reduce the ram air to reach the Pareto frontier. For the pressure ratio of the turbine-1, it tends to cluster at its lower bound. Since there are two turbines in total and concentrating more power in one turbine can reduce the pack mass, as the power-to-weight ratio increase as the turbine power increases. Meanwhile, there is a constraint that the temperature of the flow station where turbine-1 exit flow and turbine-1 bypass flow mixes has to be greater or equal to 34 °F (constraint C3). Reducing the pressure ratio of turbine-1 makes it easier to meet this constraint. Therefore, the pressure ratio of turbine-1 is clustered to its lower bound.

VI. MDP Sizing Methodology Validation Approach

The approach to demonstrate the capability of the proposed MDP sizing methodology is discussed in this section. To validate the proposed approach: the performance requirements and operation constraints have to be satisfied; the ECS performance along mission points such as ram air requirement schedule should be compared with the one sized on a single design point; and the ECS sizing effects on the mission-level metrics such as mission block fuel should be compared against the one sized on a single design point. Both ECS sized by SDP and MDP sizing method obtain the design variables from the optimization process described in Sec. V. The aircraft selected to perform such analyses is a Large Twin-aisle Aircraft (LTA), whose specification can be found in the authors' previous work [29], with some design information relevant to this work summarized in Table 6.

Table 6 Design information of selected aircraft

Parameters	Value
Passenger capacity	305
Design payload weight, lbm	64 050
Design range, nmi	7500
Cruise Mach number	0.840
Maximum cruise altitude, ft	43 000
Maximum payload weight, lbm	125 500

A. Requirements and Constraints Satisfaction Validation

Points that can represent the working conditions of the ECS in a mission are selected to validate the requirements and constraints satisfaction. These points are selected the same as in Fig. 6, as the working conditions of these points include ground, hot day condition, climb, and high altitude cruise. An analysis of an integrated model of engine, the ECS, and the cabin, which was constructed by Shi [11], is performed to predict the ECS performance. The data flow inside the integrated model is shown in Fig. 11 which illustrates how the flight conditions and heat loads influence the execution of the integrated model. The performance of the all points in the selected mission will be compared to the given requirements and constraints, where the performance is predicted by the ECS model that is sized by MDP sizing methodology.

B. ECS Performance along Mission Points Validation

The design mission specified in Table 6 for the selected aircraft is chosen to compare the performance of the ECS that is sized by SDP and MDP sizing method. The mission profile is illustrated in Fig. 12. The required ram air of both ECS is compared to demonstrate that the ECS sized by MDP sizing method is more efficient through the whole mission.

C. Mission-Level Performance Assessment

The impact on mission-level performance by the proposed MDP sizing method is assessed by comparing mission-level metrics such as mission fuel consumption. As stated in Sec. V, the impacts on mission-level metrics are caused by

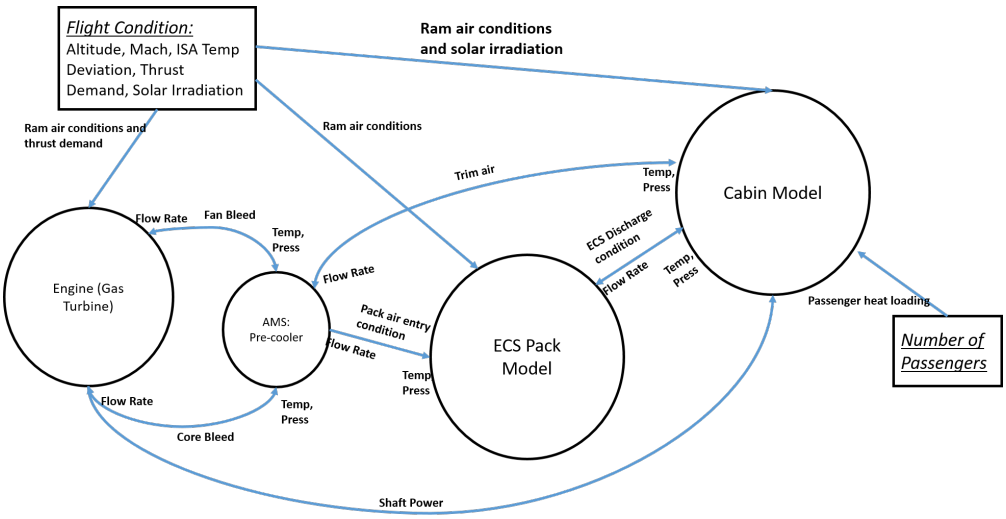

Fig. 11 Data flow of integrated engine, ECS, and cabin [11]

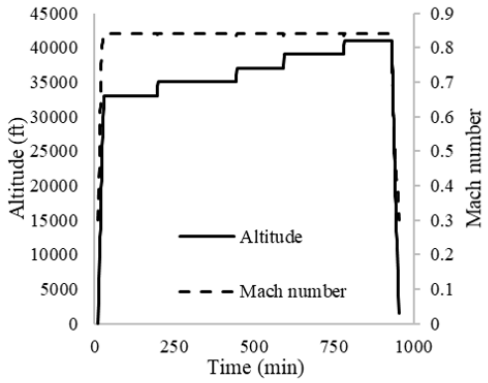

Fig. 12 Mission profile selected for requirements and constraints validation

variation in ECS weight and ram air requirements. The drag increment caused by the ram air is added to the vehicle's drag polar computed without ECS. The ram drag is computed assuming a total loss of its momentum through the inlet:

$$D_{\text{ram}} = \dot{m}_{\text{ram}} V_{\infty}$$

where V_{∞} is the freestream speed.

To ensure the vehicle point performance is invariant and its design mission requirements are met, the vehicle is resized for the design mission, maintaining the original design thrust-to-weight ratio and wing loading with the updated ECS pack mass and ram drag. The vehicle sizing and off-design mission performance evaluation is conducted using the Aircraft Sizing and Off-Design Mission Analysis Tool [29], which uses empirical component weight and drag build-up method from NASA's Flight Optimization System (FLOPS) software [30] to compute the basic vehicle empty weight and drag polar. SODA provides an interface to specify the mass of ECS packs and drag increment due to ram air intake as a function of altitude and Mach number.

VII. Results and Analysis

A. Performances of Points Constraints

The constraints and requirements applied in this MDP sizing process are already shown in Table 2. As a reminder, they are presented here again in the following table:

Performance Requirements and Operation Constraints

Independents	Dependents	Explanation
$\dot{W}_{\text{Supply\_Bleed}}$	$\dot{W}_{\text{Supply\_Cabin}}$	C1: Bleed extraction to ensure fresh cabin air $\geq 0.55\,\text{lb/person/min}$
$T_{\text{Discharge\_ECS}}$	$T_{\text{Supply\_Cabin}}$	C2: ECS pack discharge T to ensure Cabin supply T $\geq 40\,^{\circ}\text{F}$
BPR_{TCV-1}	$T_{\text{Conr\_Cold}}$	C3: TCV-1 bypass ratio to ensure condenser cold entry temperature $\geq 34\,^{\circ}\text{F}$
BPR_{TCV-2}	$T_{\text{Cmp\_Exit}}$	C4: TCV-2 bypass ratio to ensure Compressor exit temperature $\leq 260\,^{\circ}\text{F}$
BPR_{TCV-2}	$T_{\text{Ram\_Nozzle}}$	C5: TCV-2 bypass ratio to ensure ram air nozzle temperature $\leq 250\,^{\circ}\text{F}$

In this study, the total supply air is strictly set to the minimum required amount, which is $0.55 \times n_{\text{passengers}}$ lb/min, and half of this value for each ECS pack (two ECS packs in total for the selected aircraft). The cabin supply temperature is strictly set to 40 °F. Assuming that the cabin temperature is kept constant through the mission, the discharge temperature from the ECS pack is also constant through the mission. Therefore, these two constraints are guaranteed satisfied even without solving the constraint equations, and there is no need to plot these two constraints. Thus, only the actual temperatures of constrained flow stations from C3 to C5 are plotted in Fig. 13 with the constraint values, where the flight conditions are the same as in Fig. 6. The bypass ratios of TCV-1 and TCV-2 which are to control the temperatures of these flow stations are also plotted in Fig. 14.

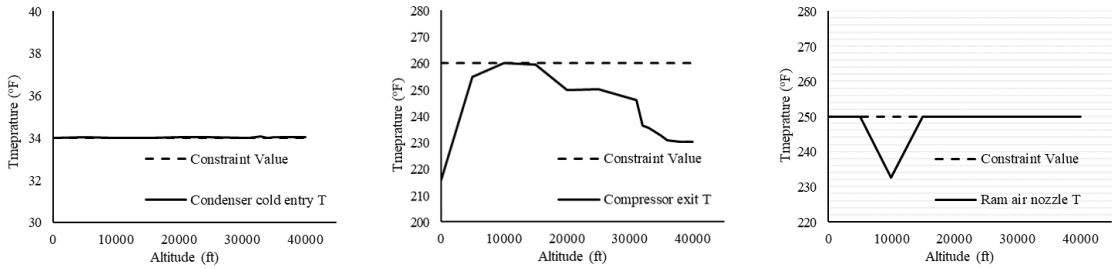

(a) Condenser cold entry temperature vs. constraint value (C3)

(b) Compressor exit temperature vs. constraint value (C4)

(c) Ram air nozzle temperature vs. constraint value (C5)

Fig. 13 Actual values at constrained flow stations vs. constraint values

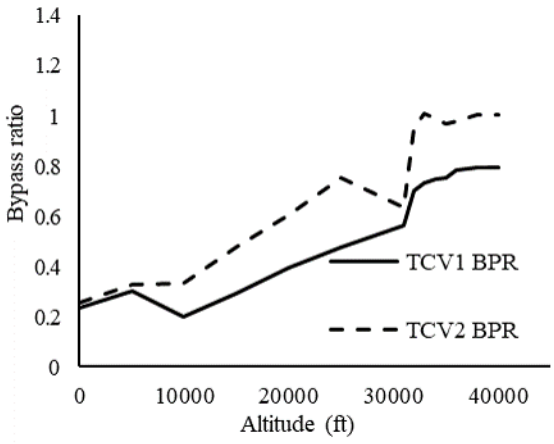

Fig. 14 Bypass ratios of TCV-1 and TCV-2 along the mission

It can be seen from Fig. 13 that the three constraints (C3, C4, and C5) are satisfied for all the selected flight conditions. In Fig. 13(a), it shows that the minimum temperature constraint of the condenser cold entry is always active.

The temperature at this flow station is controlled by bypass ratio of TCV-1. As Fig. 14 indicates, the bypass ratio of TCV-1 increases as the aircraft climbs to the cruise condition. This is because the temperature before the first turbine (Trb-1) becomes colder as aircraft flies higher, since the ambient temperature drops as altitude increases, which can absorb more heat through the primary and secondary heat exchangers. Thus there is a need to increase the bypass ratio to reduce the amount of work extracted by the Trb-1. From Fig. 13(b) and Fig. 13(c), it can be discovered that for some flight conditions the constraint for compressor exit temperature (C4) is active, while for other conditions the nozzle temperature constraint (C5) is active. As altitude increases, the main active constraint becomes C5 because the compressor exit temperature moves away from its constraint while the C5 keeps active. This is also because that at high altitude more heat will be exchanged to the ram air. Thus the bypass ratio of TCV-2 has to increase to reduce the work supplied to the compressor to reduce the amount of heat that is transferred in the secondary heat exchanger, which can be also seen in Fig. 14. In summary, the proposed MDP sizing methodology has been demonstrated to be capable of handling the ECS operation requirements and constraints.

B. ECS Performance for a Selected Mission Profile: Impacts on Ram Air

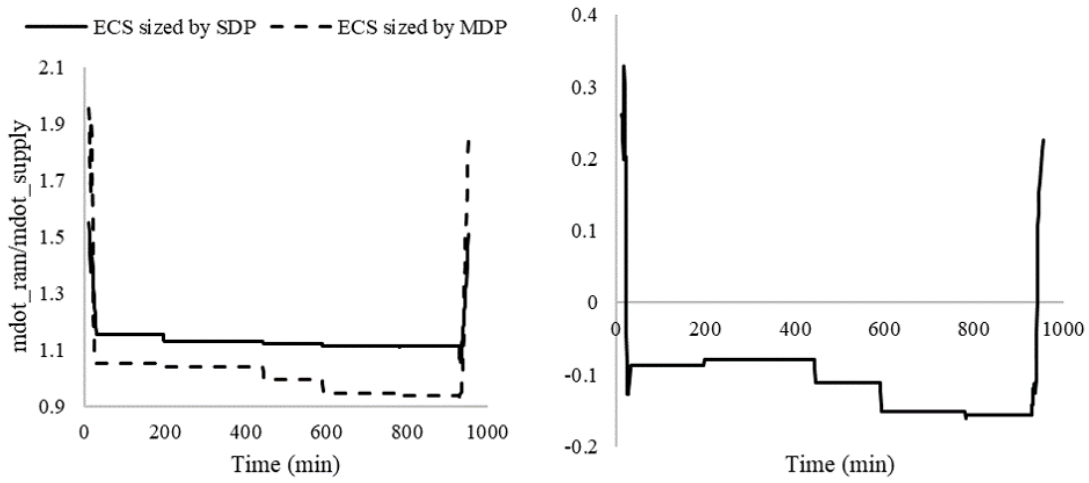

(a) Normalized ram air requirement of ECS sized by SDP and MDP (b) Relative difference between ECS sized by SDP and MDP

Fig. 15 Comparison of required ram air between ECS sized by SDP and MDP

The design mission, as shown in Fig. 12, is chosen to perform system-level comparison between the ECS sized by SDP and MDP. The required ram air for these two differently sized ECS for the selected mission is shown in Fig. 15(a), which is normalized by the amount of supply air. The relative difference of the required ram air between the ECS sized by MDP and SDP is also illustrated in Fig. 15(b). From both figures, it is shown that at the first and last several minutes when the flight altitude is low, the ram air required by the ECS sized by MDP is higher than the ECS sized by SDP, while at other points, the amount of ram air for MDP ECS is lower than that of the SDP ECS. This can be explained by the fact that all the components of the SDP ECS are sized on ground, which may lead to a design with better performance at low altitude and low Mach number. Thus it is expected that the SDP ECS should have a better performance than the ECS that is sized on other points. However, as altitude and Mach number increase, the performance of SDP ECS is then degraded. The ECS sized by MDP method takes advantage of sizing the turbomachines at the cruise condition, therefore, the MDP ECS is expected to perform better at high altitude which occupies most time of a mission. At the same time, for the MDP ECS, the heat exchangers are sized on ground, which will reduce the heat transfer penalty caused at low altitudes which might caused by moving away from the sizing condition. It can be seen from Fig. 15(b) that the maximum additional required ram air is only around 0.3 compared to the SDP ECS. It only takes 8 min after takeoff for the required ram air of the MDP ECS to be the same as that of the SDP ECS. Therefore, these discoveries have validated the capability of the MDP sizing method to size an ECS that can perform efficiently through the whole mission.

C. Mission-Level Performance: Impacts on Vehicle Sizing and Fuel Performance

The result of vehicle resizing shows that the maximum takeoff weight with MDP ECS is approximately 0.055%, or 360 lbm, lower than that with SDP ECS. The impact on range capability is illustrated in Fig. 16(a), which shows that MDP ECS has slightly decreased range capability at heavy payload and slightly increased ferry range comapred to SDP ECS, but the overall impact on range capability is negligible compared to the order of magnitude of design range. The impact of sizing method on fuel consumption is illustrated in Fig. 16(b), where the contours show the difference in block fuel of MDP ECS relative to SDP ECS within the intersection of both payload-range envelopes. The estimated fuel saving of MDP ECS is insignificant even if the ram air reduction reaches as high as 15% as shown in Fig. 15(b), since the total ram drag caused by the ECS is only around 1% of the total drag of the vehicle, and a reduction of 10% ram air mass flow will lead to around 0.1% reduction of vehicle drag and therefore block fuel. However, such savings are caused by only modifyling the sizing process and sizing conditions, thus it is enough to demonstrate the capability of the MDP sizing methodology to size an ECS that can perform multiple missions effectively.

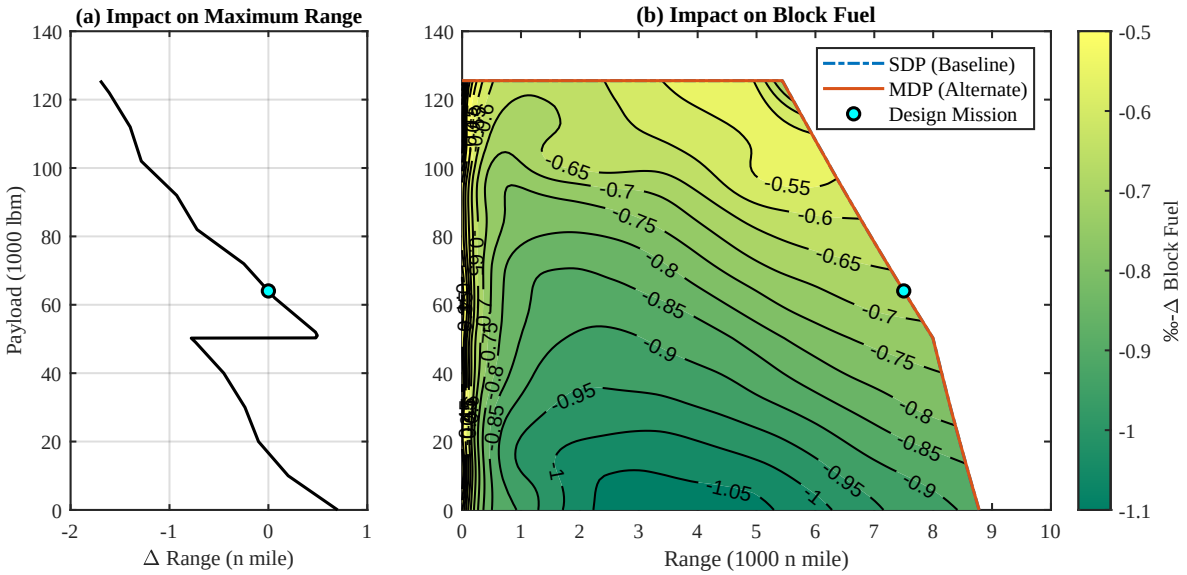

Fig. 16 Comparison of range capability and fuel consumption

Another observation from simulation data is that, while the absolute block fuel saving increases as the off-design mission range increases, the trend of relative reduction (Fig. 16(b)) is different. This phenomenon can be explained by the fact that although the more fuel is saved for higher mission ranges, the total drag of the aircraft also increases as range and payload increase because more weight is added to the aircraft. The relative reduction of the ram drag could become smaller. Therefore, larger reduction of mission block fuel is found at missions with shorter range and lower payload.

VIII. Conclusions and Future Work

This paper proposes a Multi-Design Point Sizing Methodology for the ECS, which is capable of sizing each component at its most suitable sizing condition as well as ensuring the performance requirements and constraints are satisfied through all mission points. Such capability is achieved by converting the design relations, requirements and constraints among different design points into a set of non-linear equations which is to be solved through the design process. A multi-objective optimization using Genetic Algorithm is also performed to obtain the optimal design variables to size the ECS. To reduce the computational cost of each iteration of the optimization, an artificial neural network surrogate model of the ECS is used to predict the performance in terms of the different values of design variables. The uncertainty of this surrogate model is less than 1% through validation, indicating the chosen form of the artificial neural network is suitable to represent the ECS.

The results shown in this paper validate that the ECS sized by the MDP sizing method can satisfy all the requirements and constraints at critical operating conditions. At system level, it also demonstrates that the ECS sized by the MDP sizing method can operate more efficiently than the one sized by the SDP sizing method in terms of required ram air. At

the mission level, the ECS sized by the MDP is also proved to have advantages over the SDP ECS in terms of block fuel for all the missions with different payloads and ranges. Therefore, it can be concluded that the proposed MDP sizing method is capable of sizing an ECS function efficiently through the whole mission as well as satisfying all requirements and constraints at all operating conditions.

In this paper, only the Large Twin-aisle Aircraft has been used as the example to test the ECS, which requires rather large amount of supply air due to large number of passengers. Therefore, an avenue for future work might be to research the impacts of varied supply air on the ECS sizing. The optimization objectives selected in this paper are at subsystem level, which are the required ram air and the weight. For the future work, system-level or mission-level objectives can be used to optimize the ECS design variables.

References

[1] Sinnett, M., "787 No-bleed systems: saving fuel and enhancing operational efficiencies," *Aero Quarterly*, Vol. 18, 2007, pp. 6–11.

[2] Schlabe, D., and Lienig, J., "Model-Based Thermal Management Functions for Aircraft Systems," *SAE 2014 Aerospace Systems and Technology Conference*, 2014.

[3] Pellegrini, L. F., Gandolfi, R., Silva, G., and Oliveira Jr, S., "Exergy analysis as a tool for decision making in aircraft systems design," *45th AIAA Aerospace Sciences Meeting and Exhibit*, 2007.

[4] Bender, D., "Integration of exergy analysis into model-based design and evaluation of aircraft environmental control systems," *Energy*, Vol. 137, 2017, pp. 739–751.

[5] Pérez-Grande, I., and Leo, T. J., "Optimization of a commercial aircraft environmental control system," *Applied thermal engineering*, Vol. 22, No. 17, 2002, pp. 1885–1904.

[6] Leo, T. J., and Pérez-Grande, I., "A thermoeconomic analysis of a commercial aircraft environmental control system," *Applied Thermal Engineering*, Vol. 25, No. 2, 2005, pp. 309–325.

[7] Figliola, R., Tipton, R., and Li, H., "Exergy approach to decision-based design of integrated aircraft thermal systems," *Journal of aircraft*, Vol. 40, No. 1, 2003, pp. 49–55.

[8] Rancruel, D. F., "A decomposition strategy based on thermoeconomic isolation applied to the optimal synthesis/design and operation of an advanced fighter aircraft system," Ph.D. thesis, Virginia Tech, 2003.

[9] Parrilla, J. A., "Hybrid Environmental Control System Integrated Modeling Trade Study Analysis for Commercial Aviation," Ph.D. thesis, University of Cincinnati, 2014.

[10] Chakraborty, I., "Subsystem architecture sizing and analysis for aircraft conceptual design," Ph.D. thesis, Georgia Institute of Technology, 2015.

[11] Shi, M., Chakraborty, I., Tai, J. C., and Mavris, D. N., "Integrated Gas Turbine and Environmental Control System Pack Sizing and Analysis," *2018 AIAA Aerospace Sciences Meeting, (AIAA 2018-1748)*, 2018. https://doi.org/10.2514/6.2018-1748.

[12] Shi, M., Chakraborty, I., Cai, Y., Tai, J. C., and Mavris, D. N., "Mission-Level Study of Integrated Gas Turbine and Environmental Control System Architectures," *2018 AIAA Aerospace Sciences Meeting, (AIAA 2018-1751)*, 2018. https://doi.org/10.2514/6.2018-1751.

[13] Cuifeng, Z., and Wenqiang, Y., "The general design of environment control system based on requirement analysis," *2016 IEEE International Conference on Aircraft Utility Systems (AUS)*, IEEE, 2016, pp. 1067–1069.

[14] Council, N. R., et al., *The airliner cabin environment: air quality and safety*, National Academies Press, 1986.

[15] Council, N. R., et al., *The airliner cabin environment and the health of passengers and crew*, National Academies Press, 2002.

[16] Schutte, J. S., "Simultaneous multi-design point approach to gas turbine on-design cycle analysis for aircraft engines," Ph.D. thesis, Georgia Institute of Technology, 2009.

[17] Schutte, J., Tai, J., and Mavris, D., "Multi Design Point Cycle Design Incorporation into the Environmental Design Space," *48th AIAA/ASME/SAE/ASEE Joint Propulsion Conference & Exhibit*, 2012, p. 3812.

[18] Schutte, J., Tai, J., Sands, J., and Mavris, D., "Cycle design exploration using multi-design point approach," *ASME Turbo Expo 2012: Turbine Technical Conference and Exposition*, American Society of Mechanical Engineers, 2012, pp. 271–281.

[19] Kestner, B. K., Schutte, J. S., Gladin, J. C., and Mavris, D. N., "Ultra high bypass ratio engine sizing and cycle selection study for a subsonic commercial aircraft in the N+ 2 timeframe," *ASME 2011 Turbo Expo: Turbine Technical Conference and Exposition*, American Society of Mechanical Engineers, 2011, pp. 127–137.

[20] Ypma, T. J., "Historical development of the Newton–Raphson method," *SIAM review*, Vol. 37, No. 4, 1995, pp. 531–551.

[21] Claus, R. W., Evans, A. L., and Follen, G. J., "Multidisciplinary Propulsion Simulation using NPSS," *AIAA Paper*, , No. 92-4709, 1992.

[22] Long, C., Xingjuan, Z., and Chunxin, Y., "A New Concept Environmental Control System with Energy Recovery Considerations for Commercial Aircraft," 44th International Conference on Environmental Systems, 2014.

[23] Mattingly, J. D., *Elements of propulsion: gas turbines and rockets*, American Institute of Aeronautics and Astronautics, 2006.

[24] Walsh, P. P., and Fletcher, P., *Gas turbine performance*, John Wiley & Sons, 2004.

[25] Kays, W. M., and London, A. L., *Compact heat exchangers*, McGraw-Hill, New York, NY, 1984.

[26] FAA, A., *AC 25-20-Pressurization, Ventilation and Oxygen Systems Assessment for Subsonic Flight Including High Altitude Operation*, Federal Aviation Administration, 1996.

[27] Deb, K., *Multi-objective optimization using evolutionary algorithms*, Vol. 16, John Wiley & Sons, 2001.

[28] Deb, K., Pratap, A., Agarwal, S., and Meyarivan, T., "A fast and elitist multiobjective genetic algorithm: NSGA-II," *IEEE transactions on evolutionary computation*, Vol. 6, No. 2, 2002, pp. 182–197.

[29] Cai, Y., Rajaram, D., and Mavris, D. N., "Multi-mission Multi-objective Optimization in Commercial Aircraft Conceptual Design," *AIAA Aviation 2019 Forum*, American Institute of Aeronautics and Astronautics, 2019. https://doi.org/10.2514/6.2019-3577.

[30] McCullers, L., *Flight Optimization System, Release 8.11, User's Guide*, NASA Langley Research Center, Hampton, VA 23681-0001, Oct. 2009.